Hindawi
Advances in Polymer Technology
Volume 2020, Article ID 8456024, 13 pages
https://doi.org/10.1155/2020/8456024

Research Article

Fabrication & Characterization of Chitosan Coated Biologically Synthesized TiO_2 Nanoparticles against PDR *E. coli* of Veterinary Origin

Naheed Zafar,[1] Bushra Uzair ,[1] Muhammad Bilal Khan Niazi,[2] Shamaila Sajjad,[3] Ghufrana Samin,[4] Muhammad Javed Arshed,[5] and Sikander Rafiq [6]

[1]*Department of Biological Sciences, International Islamic University Islamabad, Islamabad, Pakistan*
[2]*Department of Chemical Engineering, SCME, National University of Science and Technology (NUST), Islamabad, Pakistan*
[3]*Department of Physics, International Islamic University Islamabad, Islamabad, Pakistan*
[4]*Department of Chemistry, University of Engineering and Technology Lahore, Faisalabad Campus, Pakistan*
[5]*National Veterinary Laboratory, Ministry of National Food Security and Research, Government of Pakistan, Park Road, Islamabad, Pakistan*
[6]*Department of Chemical Polymer & Composite Materials Engineering, University of Engineering and Technology, Lahore, New Campus, Pakistan*

Correspondence should be addressed to Bushra Uzair; bushra.uzair@iiu.edu.pk

Received 10 July 2019; Accepted 21 November 2019; Published 20 January 2020

Academic Editor: Sébastien Déon

Treatment of pandrug resistant (PDR) *Escherichia coli* strain is the leading causative agent of bovine mastitis worldwide. Hence, becoming a potential threat to veterinary and public health. Therefore, to control the infection new nontoxic, biocompatible antimicrobial formulation with enhanced antibacterial activity is massively required. Current study was planned to synthesize chitosan coated titanium dioxide nanoparticles (CS-NPs coated TiO_2). Coating was being done by chitosan nanoparticles (CS-NPs) using ionic gelation method. Aqueous solution of *Moringa concanensis* leaf extract was used to synthesize titanium dioxide nanoparticles (TiO_2 NPs). The synthesized nanoformulations were characterized by using XRD, SEM, and FTIR. X-ray diffraction (XRD) analysis indicated the crystalline phase of TiO_2NPs and CS-NPs coated TiO_2 NPs. Scanning Electron Microscopy (SEM) confirmed spherical shaped nanoparticles size of chitosan NPs ranging from 19–25 nm and TiO_2 NPs 35–50 nm. Thesize of CS-NPs coated TiO_2 NPs was in the range of 65–75 nm. The UV-Vis Spectra and band gap values illustrated the red shift in CS-NPs coated TiO_2 NPs. Fourier transform infrared (FTIR) spectroscopy confirmed the linkages between TiO_2 NPs and chitosan biopolymer, Zeta potential confirmed the stability of CS-NPs coated TiO_2 NPs by showing 95 mV peak value. *In-vitro* antibacterial activity of CS-NPs coated TiO_2 NPs and Uncoated TiO_2 NPs was evaluated by disc diffusion method against PDR strain of *E. coli* isolated from mastitic milk samples. The antibacterial activity of all the synthesized nanoformulations were noted and highest antibacterial activity was shown by CS-NPs coated TiO_2-NPs against pandrug resistant (PDR) *E. coli* strain with the prominent zone of inhibition of 23 mm. Morphological changes of *E. coli* cells after the treatment with MIC concentration (0.78 μg/ml) of CS-NPs coated TiO_2 NPs were studied by transmission electron microscopy TEM showedrigorous morphological defectand has distorted the general appearance of the *E. coli* cells. Cytotoxicity (HepG2 cell line) and hemolytic (human blood) studies confirmed nontoxic/biocompatible nature of CS-NPs coated biologically synthesized TiO_2 NPs. The results suggested that biologically synthesized and surface modified TiO_2 NPs by mucoadhesive polysaccharides (e.g. chitosan) coating would be an effective and non-toxic alternative therapeutic agent to be used in livestock industry to control drug resistant veterinary pathogens.

1. Introduction

Mastitis is the most common disease of livestock and the basic reason in which animals are treated with antibiotics [1, 2]. Worldwide this is known as the most prevailing and costly disease of dairy industry and can be caused by a variety of pathogens. *E. coli* is one of the major causative agents of mastitis [3, 4]. Food producing animals are measured as key basins

of antibiotic-resistant bacteria. Whereas, unwise use of antibiotics in food industry resulted in global menace of antibiotic resistance (ABR) as bacteria cannot recognize geographic borders to hamper the worldwide spread of antibiotic resistance [5]. The appearance of ABR in the food chain is measured a cross-sectorial problem and the drug resistant strains particularly pan drug resistant or superbugs are matter of great concern [6]. PDR is defined as non-susceptibility to all agents in antimicrobial categories. The magnitude of antimicrobial resistance in *E. coli* strains is increasing because of their fast tendency to acquire resistance [5–7]. To control the issue of development of antibiotic resistance, use of antibiotics in food industry is been banned in various countries but the ban of in-feed use of antibiotics has resulted unintended in the increase of infections in animals and the decrease of animal production resulted great economic loss. Alternative nontoxic formulations are required to conquer the issue of antibiotics in food industry. Hence, the study is been planned to synthesize alternative formulation to kill superbugs in food industry.

The development of sustainable bio-based polymers with antimicrobial properties is now considered as promising alternative to control issue of antibiotic resistance among microorganisms. There are ample and outstanding research data regarding antimicrobial polymeric materials where amalgamation with antimicrobial organic and inorganic compounds are explored for controlling drug resistance. These finding showed great potential of sustainable polymeric materials as alternative antimicrobial material [8, 9]. Chitosan (CS), a linear polysaccharide having inherent antimicrobial potential is known as the most common biopolymer on earth. It provides various advantages i.e. natural, biocompatible, biodegradable, and nontoxic for mammalian cells, and has been approved by the U.S. Federal Drug Administration (FDA) and the E.U. as safe (GRAS, Generally Recognized As Safe) to be used in health care [9, 10]. A vastly searched approach for enhancing the antibacterial potential of chitosan is the amalgamation of metal-oxides [11–13]. Antimicrobial activity of TiO_2 was reported first time in 1985 by Matsunaga and colleagues [14]. They observed under illumination with near UV light that microbial cells could be killed by the contact with a TiO_2–Pt catalyst [14, 15]. According to literature, highly reactive oxygen species (ROS) are considered to be the key species in the photocatalytic disinfection process [16]. In recent years, the synthesis of nanoparticles using green approach has been increased. There are reports on the synthesis of TiO_2 nanoparticles using different plants extracts [17, 18]. The *Moringa genus* has traditionally been widely used to improve health and well-known for their antioxidant, anti-inflammatory, anticancer, and antihyperglycemic activities [19]. Most of the biological activity was caused by their high content of flavonoids, glucosides, glucosinolates, β-sitosterol and β-sitosterol-3-O-β-D-glucoside. The flavonoids are the main constituents responsible for reducing the metal precursor. According to our best knowledge no previous research was reported on the synthesis of TiO_2 by using *M. concanensis* leaf extract and extensive study on the antibacterial potential of nanoparticles synthesized using *Moringa*.

Hence the aim of the present study is to introduce a new and unique CS-NPs coated TiO_2 NPs prepared by the modified ionic gelation method. The TiO_2 NPs coated with NPs of chitosan biopolymer has endorsed its antibacterial activity against PDR strains of *E. coli* causing mastitis. Subsequently, the synthesized CS-NPs coated TiO_2 NPs were structurally characterized byusing X-ray diffractometer (XRD), FTIR spectroscopy, TEM, and SEM. Their corresponding energy dispersive X-ray analysis (EDX), UV Vis analysis, Zeta potential, particle size distribution and various bio assays i.e. disc diffusion method, growth kinetics, cytotoxicity and hemolysis studies were also conducted. There is passionate hope for battling against gram-negative PDR strains of *E. coli* causing mastitis in the livestock animals of Pakistan.

2. Materials and Methods

2.1. Materials Used. Titanium tetra isoproxide 97%, Chitosan (medium molecular weight, Product number 448877, Penta sodium tripolyphosphate (TPP) and glacial acetic acid were acquired from Sigma–Aldrich. Antibiotic discs were received from Oxoid. Chemicals were supplied and used without further purification. Double distilled water is used throughout the experiment.

2.2. Sampling and Isolation of Mastitis Causing E. coli Strains. The research was conducted in Bacteriology Laboratories of National Veterinary Laboratories, Islamabad. All the glass wares required in research were washed with distilled water and autoclaved at a temperature of 121°C, and a pressure of 15 lb/inch^2 for 15 minutes. Reagents were prepared in distilled water. In the study, 250 milk samples were screened for the detection of mastitis by surf field mastitis test [20]. Mastitic milk samples were screened for the isolation of *E. coli* on the MacConkey agar media. The identification of *E. coli* was done by using API 10S. Different test panels were prepared in dehydrated forms which were reconstituted upon use by addition of bacterial suspensions. After incubation, positive test results were scored as a relevant cumulative profile software (API ^{TM} WEB version 1.3).

2.3. Antibiotic Sensitivity Profiling of Isolated Strains of E. coli. After identification of *E. coli* antibiotics, sensitivity test (AST) was performed by using disc diffusion method.The interpretations were made as per the zone size according to CLSI guideline. A bacterial suspension of the test organism was made in 0.85 percent normal saline solution by using a sterile inoculating loop. The turbidity of the suspension was matched with 0.1 percent McFarland standard. To make the uniform bacterial lawn 5μl of suspension was seeded over the surface of Muller Hinton Agar (MH agar oxide) plate with the help of sterile cotton swab. Commercially available discs of antibiotic were used, Ceftazidime (CAZ 30 μg), Cefazolin (KZ 30 μg), Cefotaxime (CTX 30 μg), Imipenem (IPM), Cefepime (FEP), Cefoxitin (FOX 30 μg) Ceftriaxone (CRO 30 μg), Aztreonam (ATM 30 μg), Ampicillin (AMP 25 μg), Vancomycin (VA 30 μg), Meropenem (MEM 10 μg), and Augmentin (AMC 30 μg). The antibiotic discs were placedin the aseptic environment by disc dispersion and incubated for

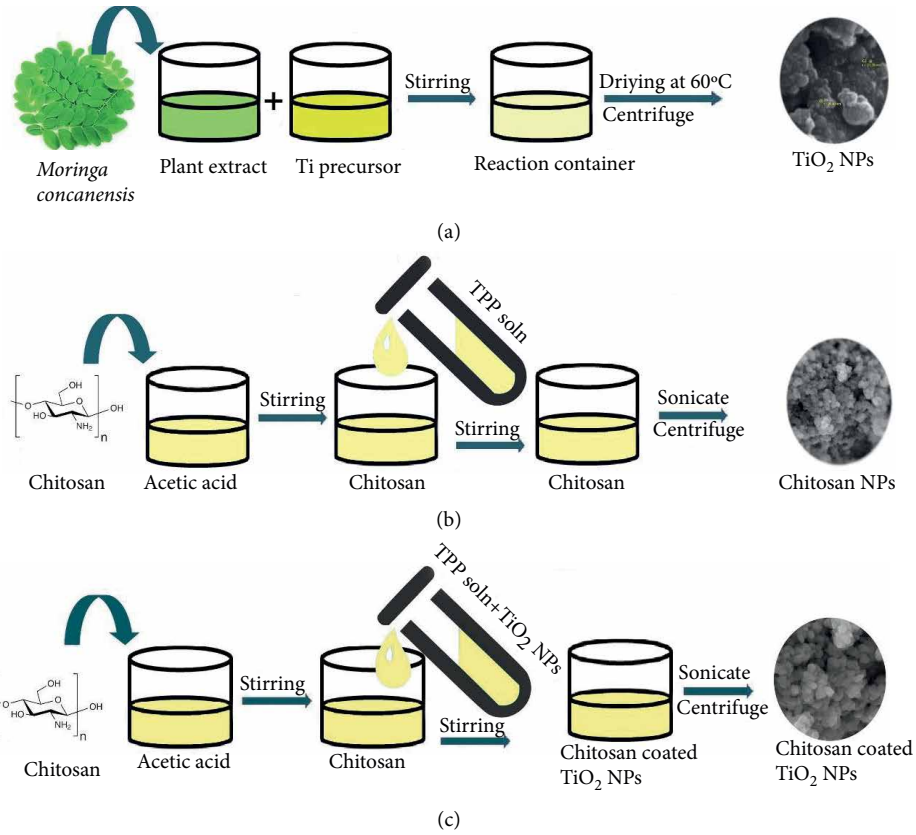

Figure 1: Crucial steps involved for synthesis of Nano antimicrobial agents. (a) synthesis of TiO_2 NPs, (b) Chitosan NPs, (c) Chitosan coated TiO_2 NPs.

24 hrs at 37°C. After 24 hrs of incubation, zone of inhibitions were recorded with the help of a measuring scale and compared with CLSI guidelines [21, 22].

2.4. Synthesis of Nanoformulations

2.4.1. Step A. Green Synthesis of TiO_2 Nanoparticles. *Moringa concanensis* leaf extract was used for the synthesis of TiO_2NPs ascribing to its medical effectiveness (Figure 1). The fresh leaves of *M. concanensis* were collected from the Hoon village of district Rawalpindi, Pakistan. Firstly leaves were washed with the tap water to remove debris and other contaminated organic contents then washed with distilled water and dried at room temperature. Approximately, 20 g of the finely cut leaves were dissolved into 200 ml distilled water in a beaker and kept on boiling for 40 minutes on a hot plate. The extract was cooled down at room temperature and filtered with Whatmann filter paper. Titanium tetraisoproxide solution was prepared in 100 ml of 0.4 M under magnetic stirring at room temperature. Under mild magnetic stirring, about 5ml of leaf extract was added to the titanium tetraisoproxide solution. The prepared mixture was centrifuged 3–5 times at 10000 rpm for 15 minute to remove the unreacted ions. Final product was dried at 60°C, ground and calcinated at 500°C in muffle furnace (Protherm furnace PLF 120/7) for about 3 hours to obtain pureTiO_2 NPs.

2.4.2. Step B. Preparation of CS-NPs. CS-NPs were prepared using ionic gelation process with few modifications [20]. Two solutions were synthesized; (1) Chitosan (CS solution A) and (2) tripolyphosphate (TPP solution B) (Figure 1). CS solution A was developed by mixing 0.3 g CS in 1% acetic acid of 100 mL solution. The solution was left to stir for homogenous clear solution. The TPP solution B was developed by adding 0.1 g TPP in 100 mL water. 4 mL TPP solution B was then added drop wise to CS solution A (100 mL) while stirring. Chitosan nano-particles (NPs) was instantly produced by the addition of TPP aqueous solution B and the blend was left to stir for 2 hrs at room temperature. Ultra-sonication was done @ 35 Hz for half hour on ice bath to maintain temperature followed by centrifugation @ 10000 g for 15 min at 4°C [23].

2.4.3. Step C. Preparation of CS-NPs Coated TiO_2 NPs. As shown in Figure 1, for the coating of CS-NPs, CS Solution A was kept on constant stirring at room temperature for 30 min. TPP Solution B containing TiO_2NPs was added dropwise in the CS solution A. The NPs were sonicated by ultra-sonication at 35 Hz for at least 30 min on the ice bath to maintain the temperature and was centrifuged at 10000 g for 15 min at 4°C. Supernatant was discarded and pallet was air dried for further experiments [23].

2.5. Structural Characterization of Synthesized Nanoformulations. X-ray diffraction patterns of TiO_2 NPs were taken

in the range of 10–80° (2θ) using wide angle XRD using (Cu Kα1 radiation, λ = 1.5406 Å), operated at 40 kV and 100 mA.

Fourier transform spectroscopy (FT-IR Perkin Elmer Spectrum 100 spectrometer) was used to determine the functional group and the unknown elements present in the samples.

UV visible spectroscopy was performed by using "Scan UV-Vis–NIR spectrophotometer" equipped with an integrated sphere assembly, using $BaSO_4$ as a reflectance sample.

Scanning electron microscopic photographs and energy dispersive X-ray spectra were observed by S-4700 Hitachi, Japan.

TEM (JEOL JEM 1010) was used to study morphological changes on bacterial cells after treating with CS-NPs TiO_2 NPs.

Zeta potential is the charge on the diffused aqueous layer formed on nanoparticles surface when it suspended in water. Zeta potential and particles size of chitosan NPs, TiO_2NPs and CS-NPs coated TiO_2 NPs were measured at room temperature through Malvern zeta sizer.

2.6. Antibacterial Effect and MIC Determination of CS-NPs Coated TiO_2 NPs on PDR Strain of E. coli. Disc diffusion method of Guzmán et al. was employed [24] to examine antibacterial activity of CS-NPs coated TiO_2 NPs, TiO_2 NPs and chitosan NPs (DMSO as control disc). A bacterial suspension of the test organism was made in 0.85 percent normal saline solution by using a sterile inoculating loop. The turbidity of the suspension was matched with 0.1 percent McFarland standard. 5 μl of the suspension was then spread over the surface of Muller Hinton agar (MH) plate with the help of sterile swab in order to make a bacterial lawn. Paper disc were loaded with prepared nano formulations and placed aseptically on the surface of MH plate, incubated for 24 hrs at 37°C. Zone of inhibition were measured with the help of vernier calipers and experiment was repeated in triplicate for accuracy. For minimum inhibitory concentration (MIC) was performed according to protocol of [24] by taking 100 μl of bacterial suspension in the nano sized CS-NPs coated TiO_2 NPs with varying concentration of 0.01–100 μg with two fold serial dilutions. Three rounds of experiment were conducted with negative and positive control. ATCC 8739 strain of *E. coli* was taken as control organism.

2.7. Growth Curve Kinetics of PDR E. coli Strain Treated with Nanoformulations. Growth kinetics of CS-NPs coated TiO_2 NPs, TiO_2 NPs and CS NPs were determined through standard micro-dilution Broth assay of Holowachuk, et al. [25]. The bacterial turbidity of PDR *E. coli* inoculated in nutrient broth was compared to McFarland standard after 24hrs of incubation. Stock solutions of synthesized nanoformulations were prepared in sterilized nutrient broth and subjected to sonication for 15 min. Briefly, 10 μl log phase of bacterial suspension was added to 96-well plate and the volume in the 96-well plate was adjusted by adding 200 μl of sterilized broth containing MIC concentrations of synthesized nanoformulations. Reaction mixture was incubated at 37°C to measure OD values at 600 nm on ELISA Multiplate reader after every 2hrs of time interval (0–24 hrs).The experiment was run in triplicate using both positive and negative controls.

2.8. Observation of Changes in Morphology of PDR E. coli Treated with CS-NPs Coated TiO_2 NPs by TEM. Changes in the morphology of log phase cells of PDR *E. coli* treated with *CS-NPs coated TiO_2 NPs* was observed by TEM analysis Hartmann et al. protocol was followed with few modified steps [26]. After the treatment with MIC concentration of CS-NPs coated TiO_2 NPs at various intervals of time (0, 3, 6 hrs), total 10 μl of log phase *E. coli* cells were taken on the neat and clean glass slide. Untreated cells were taken as a control, cell fixation was done by glutaraldehyde (2%) and paraformaldehyde in the buffer HEPES (30 mM) for about one hour. Washing of cells was done with ethanol in the prepared diluted concentrations (30, 50, 70, 90, 95 and 99.5%) for 10 min in each grade of dilution. Then slides were soaked in the terl.butyl alcohol for one min, washed thrice and dried in the vacuum to analyze morphological changes in bacterial cells by TEM.

2.9. Cytotoxicity Evaluation. Cytotoxicity evaluation of chitosan, TiO_2 NPs and CS-NPs coated TiO_2 NPs was performed on HepG2 cell lines by MTT method of Lupu et al. procedure [27]. Dulbecco's modified Eagle medium (DMEM) was used to grow HepG2 cell lines in 96 well plate. After optimal growth of cells, HepG2 cells were treated with four different concentrations of synthesized nanoformulations (0.02 ug/ml, 0.2 ug/ml, 0.1 ug/ml, 0.3 ug/ml) considering Celecoxib as positive control and incubated at 37°C for 24 hrs. According to the protocol [27], 100ul media which are prefer to be freshly prepared, 10 μL of MTT solution and PBS buffer was made to replace the previous media after 24 hours and again incubated for 4 hours. Then 0.1 DMSO solution used to dissolve formazan crystal in the wells, OD of the plates containing MTT formazan and test sample were determined at the reference wavelength of 570 nm and 620 nm respectively. Percentage viability calculated by the given formula [27].

$$\text{Percent cell viability} = \frac{(\text{Test } 570\,nm - 620\,nm)}{(\text{Control } 570\,nm - 620\,nm)} \times 10. \quad (1)$$

2.10. Hemolysis Assay. The hemolysis assay of Choi et al.[28] was used to study the effect of CS-NPS coated TiO_2NPs on human blood cells. Various concentrations of synthesized CS-NPS coated TiO_2NPs formulation (0.78 μg/ml, 1.56, 3.12, 6.25, 12.5, 20, 50 μg/ml) was used to study hemoglobin release after treatment with nanoformulations. PBS was taken as negative control and 1% triton X-100 was taken as positive control. The absorbance was dignified at 540 nm to calculate the aggregate of hemoglobin release after treatment.

3. Results and Discussion

3.1. Sampling and Isolation of Mastitis Causing E. coli Strains. From 159 milk samples, 57 *E. coli* strains were isolated (data not shown). Antibiotics sensitivity profiling showed 27 MDR strains and PDR strain of *E. coli*. Hence, PDR *E. coli* was selected for evaluating antibacterial potential of our synthesized formulation i.e. CS NPs coated TiO_2 NPs and CS NPs.

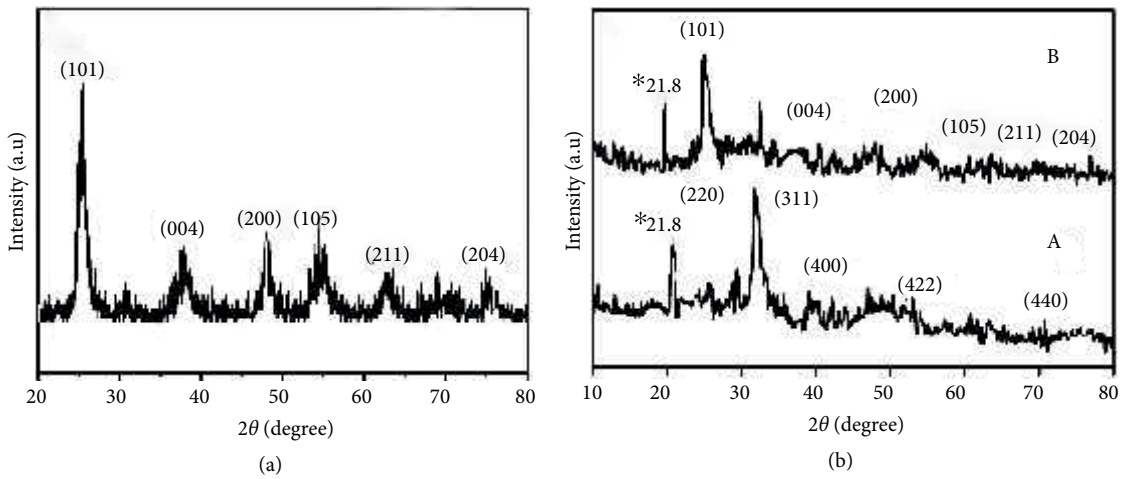

Figure 2: XRD patterns of synthesized nanomaterials: (a) TiO_2 NPs, (b) line (A) represents the chitosan and (B) CS-NPs coated TiO_2 NPs.

3.2. Structural Characterization of Synthesized Nanoformulations

3.2.1. X-Ray Diffraction Spectroscopy. XRD measurements were presenting the crystalline size and nature of synthesized nanomaterials. Figure 2(a) indicates the XRD profile of, TiO_2 NPs. XRD pattern of TiO_2 results represents the (101), (004), (200), (105), (211) and (204) plane. These planes are corresponding to crystalline anatase phase [29]. In the graph characteristic peaks indicate the anatase phase of TiO_2 without any indication of other diffraction peaks of impurity. There is a strong peak in the diffractogram of chitosan at 21.8∘, indicating the high degree of crystallinity of chitosan as shown in Figure 2(a)(B). In the Figure 2(b)(B), TiO_2 coated with CS-NPs are comprised of a dense network structure of interpenetrating polymer chains cross-linked to each other by TPP counter ions [30]. It is clear in the Figure 2(b)(B) that TiO_2 maintained its structure during coating by showing its similar characteristic peaks and plane indices.

3.2.2. Scanning Electron Microscopy and Energy Dispersive Spectroscopy Analysis. In the Figure 3(a) SEM photographs of TiO_2 showed spherical appearance while CS-NPs coated TiO_2 NPs photograph is shown in Figure 3(b). It was clearly seen from the image that nanoparticles presented spherical and agglomerated morphology. The size of nanoparticles was comprised of the diameter ranging from 19–75 nm. The size of chitosan NPs was found to be in the range of 19–25 nm, TiO_2 NPs were 35–50 nm and CS-NPs coated TiO_2 NPs ranging from 65–75 nm. The relevant data of EDX is listed in Table 1. Figures 3(c) and 3(d) indicates the signals of Ti and O which confirmed the synthesis of CS-NPs coated TiO_2 NPs and TiO_2 NPs.

3.2.3. UV-Visible Spectroscopy. UV-Vis spectrum of the TiO_2 nanoparticles, chitosan and CS-NPs coated TiO_2NPs are exhibited in the Figures 4(a) and 4(b), respectively. From the spectra, the absorption power of TiO_2 NPs, chitosan NPs and CS-NPs coated TiO_2 NPs was in the red area. This describes the CS-NPs coated TiO_2 active in the visible light due to the existence of chitosan with TiO_2 nanoparticles. Moreover, it was due to surface modification of TiO_2 by chitosan which shifted the absorption edge in visible range. The absorbance spectrum consists of two bands, one at around 220 nm and other band around 320 nm. The band around 220 nm is assigned to tetrahedral isolated Ti and the band around 300–400 nm arises due to charge-transfer from the valence band (mainly formed by 2p orbitals of the oxide anion) to the conduction band (mainly formed by 3d t_{2g} orbitals of the Ti^{4+} cations). This band further confirms the existence of the anatase phase of TiO_2 [31]. An obvious red shift towards the Vis portion of light could be attributed to addition of chitosan contents which possesses the small band gap value. This improvement in UV-Visible light absorption is demonstrating that the major portion of solar light could be successfully utilized.

Colloidal samples of the three phases were analyzed using UV–vis transmission measurements. Extrapolation of the reflectance versus wavelength curves shown in Figures 5(a) and 5(b) Results in the following estimates of the band gap energy 3.21 eV for anatase phase of TiO_2 observed. It is clearly seen that TiO_2 nanoparticles are respondent only to the UV region of light due to having wide band gap energy value. UV spectrum of chitosan manifests the absorption peak at 202 nm. In case of CS NPs coated TiO_2NPs considerably improvement was observed in absorption spectrum in UV-Vis light region. An obvious red shift towards the Vis portion of light could be attributed to the addition of chitosan content which possesses the small band gap value [30, 31].

3.2.4. Fourier Transform Infrared Spectroscopy. The FTIR spectra of TiO_2NPs, Chitosan and CS-NPs coated TiO_2 NPs are shown in Figure 6. The FTIR spectrum of the chitosan (Figure 6(a)) exhibits a sharp absorption peaks for 3423 cm^{-1} which is related to availability of free –OH group of water molecule and C=O carbonyl moieties. Chitosan characteristic adsorption bands appear at 1636 cm^{-1} which confirms the presence of N-acetyl group. The small band at 1550 cm^{-1}corresponds to N–H bending of amide II and is overlapped by other bands. The peak at 1018 cm^{-1} is corresponding to a stretching vibration from C–O–C bonds of epoxy or alkoxy. The peak at 1269 cm^{-1}

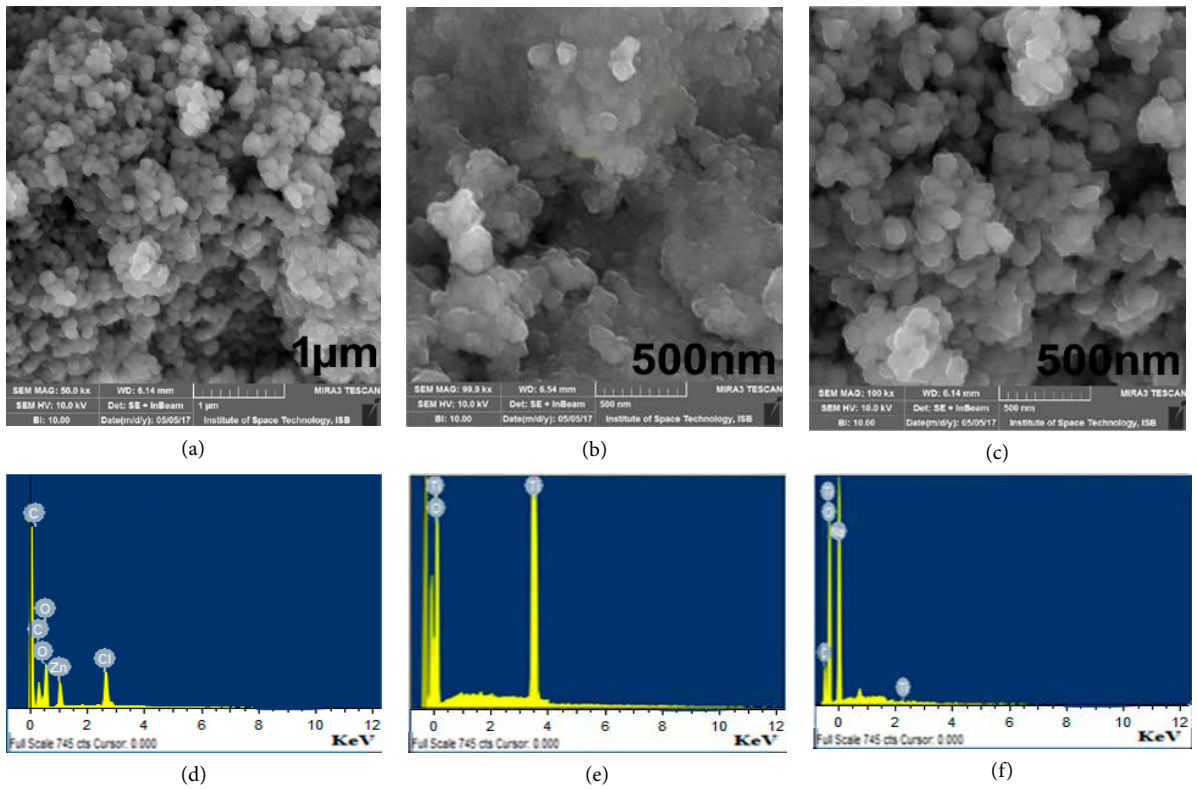

Figure 3: SEM and EDX data of synthesized formulations. (a) TiO_2NPs, (b) CS-NPs coated TiO_2NPs, (c) chitosan NPs, (d) EDX of Chitosan NPs, (e) EDX of TiO_2 NPs, (f) CS-NPs coated TiO_2 NPs.

Table 1: EDX of synthesized nanomaterials.

Samples	Weight							
Elements	Ti	O	C	Na	Ti	O	C	Na
TiO_2 NPs	50.78	49.22	—	—	25.63	74.37	—	—
CS-NPs coated TiO_2NPs	2.52	55.30	26	12.40	0.85	0.61	34.71	8.40
Chitosan NPs	—	40.57	43.72	—	—	49.75	50.42	—

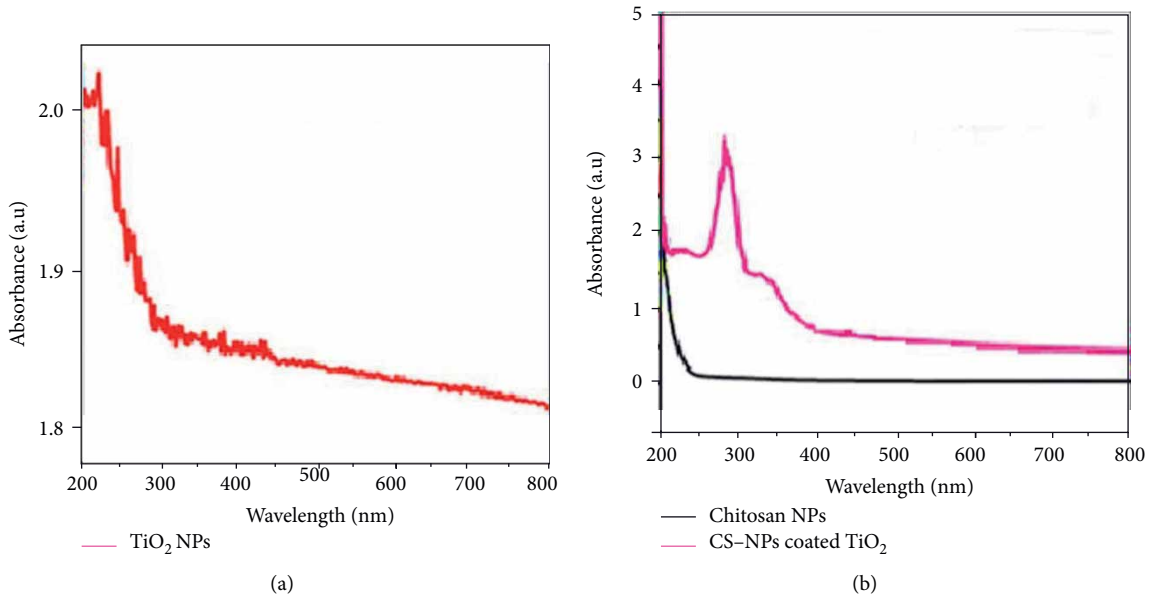

Figure 4: UV-Vis absorbance spectra of synthesized formulations. (a) TiO_2 NPs, (b) Chitosan and CS-NPs coated TiO_2 NPs.

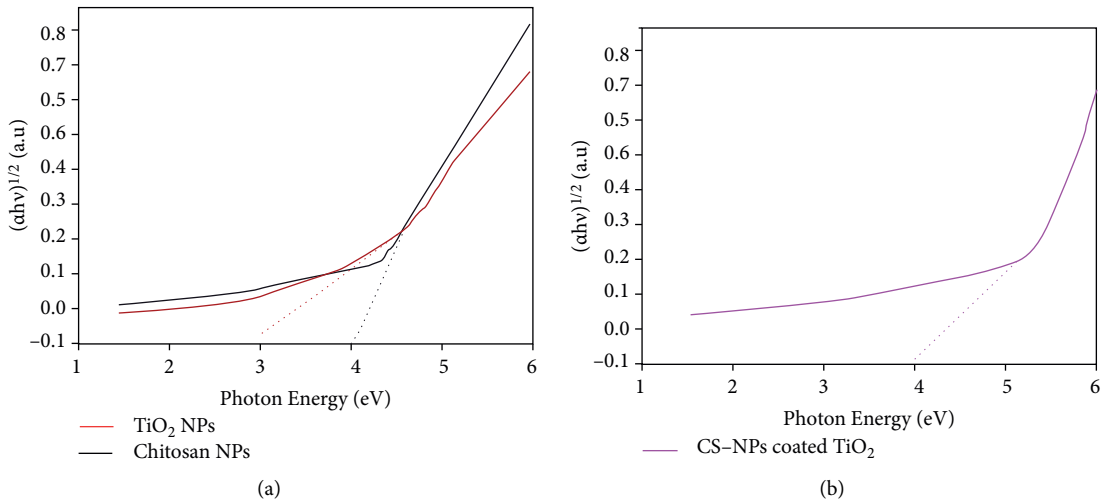

FIGURE 5: Calculations of band gap of synthesized formulations. (a) TiO_2 NPs and Chitosan NPs, (b) CS-NPs coated TiO_2 NPs.

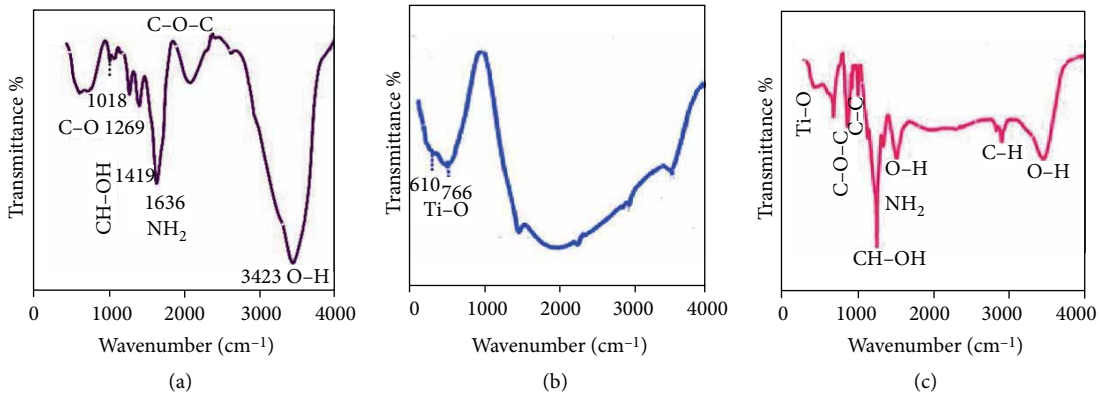

FIGURE 6: FTIR analysis of prepared nanomaterials. (a) Chitosan NPs, (b) TiO_2 NPs, (c) CS-NPs coated TiO_2 NPs.

and 1419 cm^{-1} is attributed to C–O and the CH–OH bonds, respectively. FTIR spectrum of pure TiO_2NPs (Figure 6(b)) exhibits absorption band in the range of 766–610 cm^{-1} which is related to the Ti–O bonding which authenticates the formation of TiO_2NPs. FTIR investigation of CS-coated TiO_2NPs is shown in Figure 6(c). FTIR spectrum exhibits the emergence of absorption characteristic peaks at 3408 $cm^{-1}$for hydroxyl groups. The sample also exhibits peaks related to chitosan for at 1550 cm^{-1}corresponds to N–H bending of amide II and a peak at 1018 cm^{-1} is corresponding to a stretching vibration of C–O–C bond. The peak of 665 cm^{-1} is related to the Ti–O bonding. The characterization results are in accordance to previously reported work [30, 31].

3.2.5. Zeta Potentials. The Zeta potentials of TiO_2 NPs, chitosan and CS-NPs coated TiO_2 NPs were −150.5 ± 0.8, 75.6 ± 1.0, and 95 ± 1.65 mV, respectively. The Zeta potential of prepared CS-NPs coated TiO_2 NPs were 95 ± 1.65 mV. These results provided evidence of successful coating of chitosan on the surface of TiO_2 NPs and suggested that the samples were stable during the storage period. The interaction among chitosan and TiO_2 NPs in water solution was possibly promoted by the electrostatic force as chitosan carried positive charges. Whereas, TiO_2 NPs were negatively charged furthermore, the amine groups of chitosan were protonated to ammonium thus adding the positive charges to chitosan [32–34].This phenomenon facilitated the surface coating of TiO_2 by chitosan and also prevented the aggregation of CS-NPs coated TiO_2 NPs (Figure 7).

3.2.6. Particles Size Distribution. Results of particles size distribution are shown in the Figures 8(a)–8(c). Figure 8 represents the size distributions of formulated CS-NPs coated TiO_2 NPs, Chitosan and TiO_2 NPs, respectively [35]. A group of particles (19–75 nm) was observed in all the Figures. Results showed that CS-NPs coated TiO_2 NPs were less than 80 nm, which further confirmed the stability of CS-NPs coated TiO_2 NPs. Furthermore, it indicates that chitosan is a suitable stabilizer for the surface modified preparation of metal nanoparticles. Chitosan biopolymer is used because of its shielding obstruction which can delay ripening, water loss as well as destruction of products. The current study

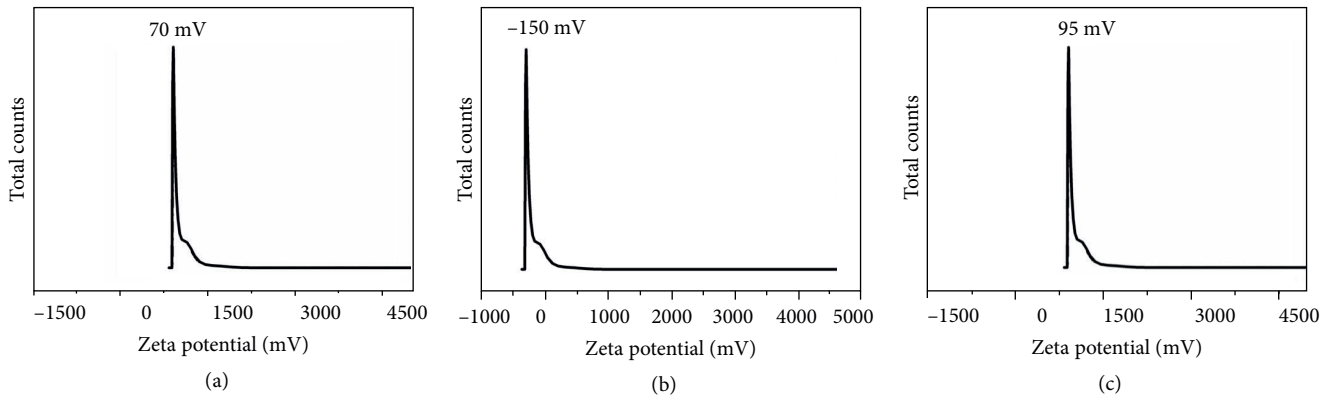

FIGURE 7: Expression of Zeta potentials of prepared nanomaterials. (a) Chitosan NPs, (b) TiO_2NPs, (c) CS-NPs coated TiO_2 NPs.

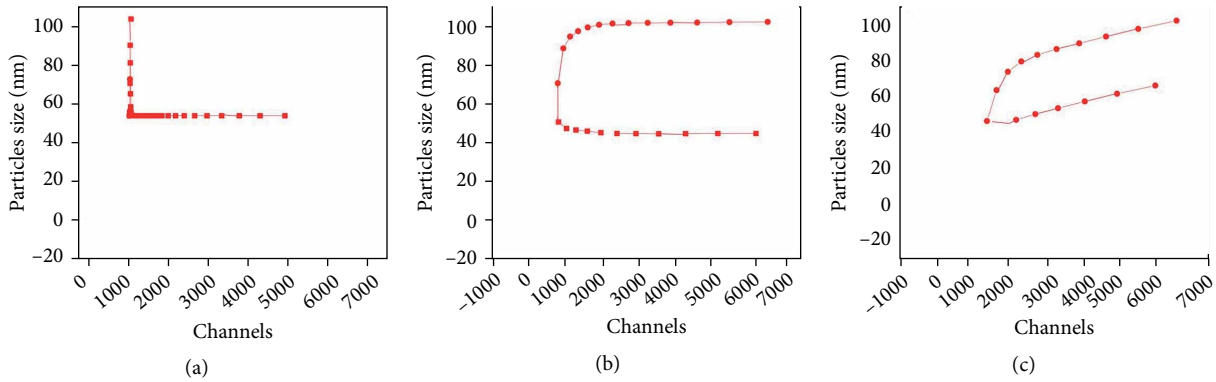

FIGURE 8: Particles size distribution of prepared nanomaterials. (a) TiO_2NPs, (b) Chitosan NPs, (c) CS-NPs coated TiO_2 NPs.

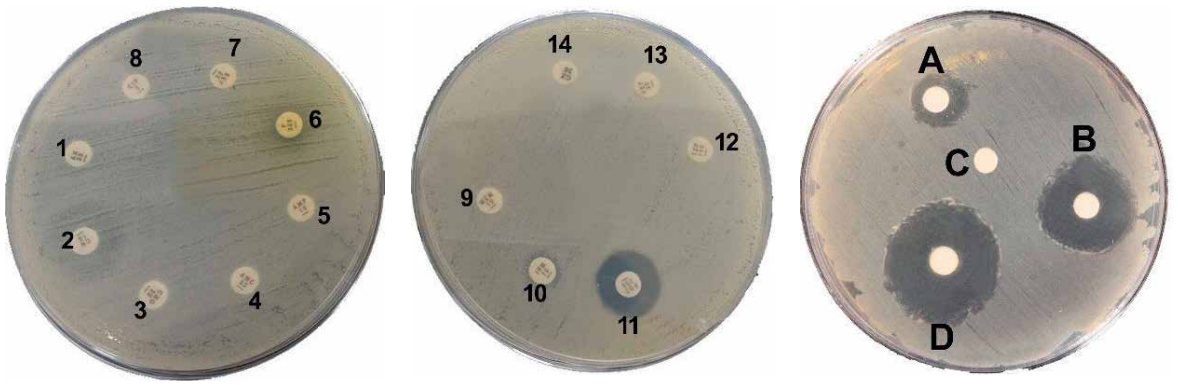

FIGURE 9: Antibiotic sensitivity profiling of isolated *E. coli* strain and antibacterial activity of synthesized nanoformulations. (a) and (b) different antibiotics discs: 1-AX, 2-CN, 3-CRO, 4-AMC, 5-AMP, 6-F, 7-SXT, 8-CIP, 9-MEM, 10-IPM, 11-FOT, 12-TZP, 13-FEP, 14-CZ, (c) Antibacterial activity of synthesized materials: A-chitosan NPs, B-TiO_2 NPs, C-control, D-CS NPs coated TiO_2 NPs.

zeta potentials values also confirmed the stability of chitosan CS coated TiO_2 NPs.

3.3. Antibacterial Effect and MIC Determination of CS-NPs Coated TiO_2 NPs on PDR Strain of E. coli. Antibiotic resistant profiling of *E. coli* strain is shown in Figures 9(a) and 9(b). The results indicate that isolated strain is found to be pandrug resistant, selected 14 antibiotic discs of commonly used antibiotics of different classes were tested and strain showed resistance against all antibiotics. Interestingly, the synthesized formulation worked against pan drug resistant *E. coli* and killed resistant strain and zones of inhibition were quite promising as seen in Figure 9(c). Synergistic antibacterial effects of some polymers and metal nanomaterials have been reported the biocidal activities of Ag and Cu NPs embedded in polymer matrices. This can be attributed to release of metal ions while tumbling their toxicities as natural polymers is biodegradable [36]. The results revealed all of three nano formulations are

Table 2: Zone of inhibition and SD values of formulated Nano antimicrobial agents.

Antimicrobial agents	Zone of inhibition (mm)	
	(ATCC 8739)	*E. coli* PDR strain
CS-NP coated TiO_2 NPs	29 mm ± 2.45	21 mm ± 0.039
TiO_2 NPs	23 mm ± 1.67	16 mm ± 2.8
Chitosan NPs	9 mm ± 0.58	4 mm ± 1.32
DMSO (control)	NZ	NZ

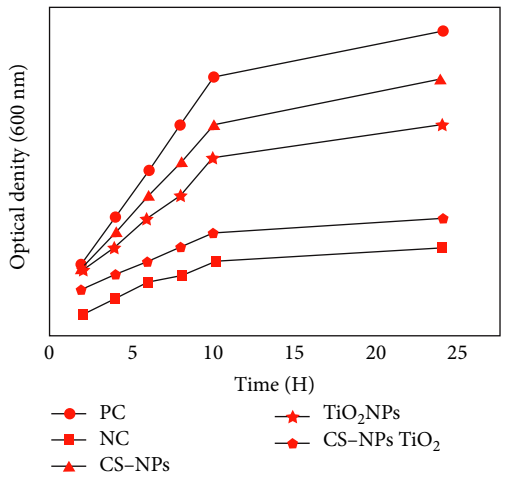

Figure 10: Growth kinetics of *E. coli* at the MIC concentrations for 24 hours. CS-NPs coated TiO_2 NPs control the bacterial growth efficiently.

effective against PDR *E. coli* but the most potent activity was noticed against CS NPs coated TiO_2 NPs. Data of zones of inhibition is presented in Table 2. MIC concentration of CS NPs coated TiO_2 NPs was found to be 0.78 μg/ml. In a study conducted by Shams and coworkers had synthesized antibacterial nanocomposites material against food borne pathogens [36]. TiO_2 NPs was found to inhibit the growth of Gram negative bacteria. The inhibition depends highly on TiO_2 NPs concentrations. Adams et al. reported that 44% reduction in the growth of *E. coli* by 1 g L^{-1} and 72% reduction by 5 g L^{-1} TiO_2 NPs [37]. Moreover Tong et al. reported 70% reduction in the growth of *E. coli* by 10 mg L^{-1} TiO_2 NPs [38]. Present study has reported low MIC value 0.78 μg/ml of CS-NPs coated TiO_2 NPs in comparison with previous findings which may be due to synergistic effect of chitosan with TiO_2 NPs and this is the possible reason for low cytotoxicity as well in current study.

3.4. Growth Curve Kinetics of PDR Strain of E. coli. According to the present study, CS-NPs coated TiO_2 NPs were found highly active in combating PDR strain of *E. coli* thanTiO_2-NPs and CS-NPs. However, CS-NPs coated TiO_2 NPs effectively dropped the OD value. Growth kinetics revealed strong antibacterial potential of synthesized CS-NPs coated TiO_2 NPs as shown in Figure 10. The antibacterial ability of chitosan was higher than that of TiO_2 NPs during the first

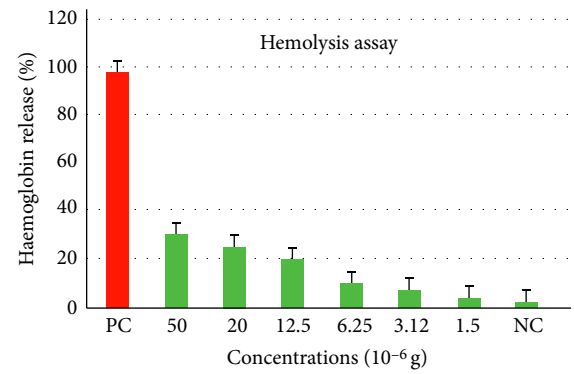

Figure 11: Hemolysis study of CS-NPs coated TiO_2 NPs after exposure to RBCs of human blood. Key: PC. Positive control, NC. Negative control.

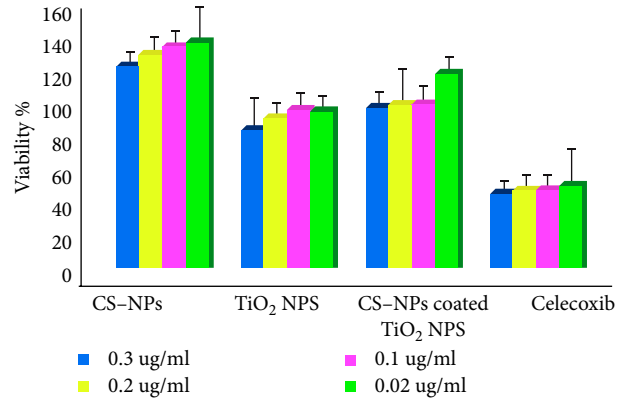

Figure 12: Cytotoxicity analysis of CS-NPs coated TiO_2 NPs, CS-NPs and TiO_2 NPs after exposure to HepG2 cell line of human.

few hours. However, the difference became insignificant over the following 5 hours. *E. coli* cells treated with TiO_2 NPs with coating of nano chitosanproved as potent coating material demonstrated relative decrease in the incubation time for the absolute lack of colony forming units of *E. coli* cells. This study showed a steady decrease of colony forming units/ml from 0 hours to ten hours as indicated in Figure 10. Hence, the time kill kinetics showed that synthesized formulation was able to kill *E. coli* as no viable cells could be recovered 10 h after exposure with CS-NPs coated TiO_2 NPs.

3.5. Hemolysis Assay. The synthesized formulations were found nontoxic to human blood cells as all formulation at various tested concentrations did not lyse red blood cells as shown in Figure 11. The hemolysis percentage indicated the compatibility of synthesized nanoformulations with human RBCs.

3.6. MTT Assay for Cytotoxicity Analysis. The cytotoxicity data exhibited in Figure 12 clearly indicates that the CS-NPs coated TiO_2 NPs, CS NPs and TiO_2 NPs did not show any toxicity on HepG2 cells at various concentrations. Results indicate that the cell viability remain maintained with the increase in concentrations of various prepared nanoformulations

and particularly CS-NPs coated TiO_2 NPs do not show any cytotoxicity on the HepG2 cell lines. Celecoxib was taken as positive control and significantly reduced cell viability at tested concentrations. All findings clearly suggest non toxicity of CS-NPs coated TiO_2 NPs may be attributed to controlled release of TiO_2 and coating of chitosan biopolymer. The preliminary results support the assumption that chitosan coatings have the potential to locally deliver antimicrobials to kill pathogens without being toxic to host cells/tissues. Sha et al. [39] analyzed cytotoxicity of TiO_2NPs using four liver cells from human and rat and found same titanium dioxide nanoparticles showed different cytotoxicity towards liver cells. The study suggested based on their experiments that the *in vitro* cytotoxicity caused by nanoparticles should be tested with great caution and there is a need to standardize the cytotoxicity testing protocol when using different cell lines. Results of this study revealed that coating with nano chitosan on TiO_2 NPs reduced cytotoxicity as presented in Figure 12.

3.7. CS-NPs Coated TiO_2 NPs Altered Morphology and Structure of PDR E. coli. Morphological changes in the integrity of PDR *E. coli* strain after treatment with MIC concentration (0.78 μg/ml) of CS-NPs coated TiO_2 NPs was studied by TEM analysis. Expected destruction of bacterial cells was observed in accordance with disc diffusion and growth kinetics assay. Both have shown antimicrobial potential. It is evident from the results (Figures 13(b) and 13(c) that CS-NPs coated TiO_2 NPs completely collapsed the PDR *E. coli* and their integrity was lost. Moreover, it was observed that shape of bacillus was no more remain maintained which may became the ultimate cause of cell deathas structural damage is clearly seen in Figures 13(b) and 13(c). From the Figure 13(c), membrane roughness or alteration in cell shape (e.g. blebbing) can be seen. Whereas, partial leakage of cellular contentis also noticeable as cells become sunken with the presence of debris representing likely intracellular leakage.

3.8. General Mechanism for the Destruction of Bacterial Cells by CS-NPs Coated TiO_2 NPs. To overcome resistance, coating of chitosan contents on TiO_2 NPs can significantly improve the bactericidal effect against PDR strain of *E. coli* causing mastitis. CS-NPs coated TiO_2 NPs were found highly effective antimicrobial agents due to the synergistic effect of the TiO_2 NPs and chitosan NPs. The TiO_2 displayed antimicrobial activity when bacterial cells exposed to it [40]. Chitosan has been reported intrinsic antimicrobial action against Gram-negative bacteria [41]. When bacterial cell treated with CS-NPs coated TiO_2 NPs as demonstrated in the Figure 14, TiO_2 undergoes the chemical reaction and generates the ROS. This play an essential role in the growth inhibition of PDR strain of *E. coli* by oxidizing polyunsaturated phospholipids of microbial cell membranes causing alterations in cellular morphology and cytoplasmic leakage [41, 42]. In Figure 14, proposed mechanism of action has been shown to describe the destruction of *E. coli* a Gram-negative bacteria. Mechanism of antimicrobial activity of synthesized formulation mainly follows three steps i.e. first step preceded after the attachment and penetration of CS NPs coated TiO_2 NPs in the bacterial cells which was facilitated by nano chitosan coating. In the second step, generation of ROS occurred after the interaction of PDR *E. coli* with CS-NPs coated TiO_2 NPs. The generation of cations by the oxidation of TiO_2 NPs and ROS are followed by the dispersion of chitosan coated nanomaterials into the growth medium under incubation during the antibacterial activity against *E. coli*. In the third step, lysis of *E. coli* cell took place due to ROS stress causing damaging of cellular content like cell wall, cell membrane, DNA and likely inhibition of protein synthesis.

Fundamental steps for the generation of ROS are described as follow

$$TiO_2 + h\nu \longrightarrow TiO_2(h^+ + e^-). \quad (2)$$

$$H_2O \longrightarrow H^+ + OH^-. \quad (3)$$

$$H^+ + OH^- \longrightarrow \cdot OH. \quad (4)$$

$$H^+ + H_2O \longrightarrow \cdot OH + H^+. \quad (5)$$

$$e^- + O_2 \longrightarrow \cdot O^{2-}. \quad (6)$$

Wang et al. and Zhu et al. reported ROS generating antibacterial TiO_2 NPs. They explored that these TiO_2 NPs have potential to increase the permeability of microbial cell membrane and induce detrimental effects inside the microbial cells, such as oxidation of intracellular Coenzyme A and lipid peroxidation, which successively cause cell death [41–43]. Gram-negative bacteria, apart from the cell membrane, possess an additional outer layer membrane, consisting of phospholipids, proteins and lipopolysaccharides, which are impermeable to most molecules [44]. Many studies also reported that Gram-negative bacteria are more resistant to antimicrobial agents because they have a triple-layered cell wall structure which contains a cytoplasmic inner membrane, a thin peptidoglycan middlelayer and an outer membrane. Thus, hinder many molecules to pass through the cell membrane [43–45]. The proposed nanoformulation, CS-NPs coated TiO_2 NPs exhibited highly efficient antibacterial activity against PDR strain of *E. coli* inspite of highly evolved resistance mechanism.

4. Conclusion

In the current study, TiO_2 NPs were synthesized using green route. Furthermore, the synthesized TiO_2 NPs were coated with nano-chitosan to enhance the effectiveness of antibacterial potential and to reduce cytotoxicity of biologically synthesized TiO_2 NPs against pan drug resistant *E. coli* causing mastitis in the livestock animals. The results revealed that synthesized formulation has superior antibacterial activity against PDR *E. coli* that has opened a new window for the alternate treatment strategy against super bugs by surface modification of TiO_2 NPs via CS-NPs. The XRD pattern of the CS NPs coated TiO_2 NPs affirmed the crystalline structure of

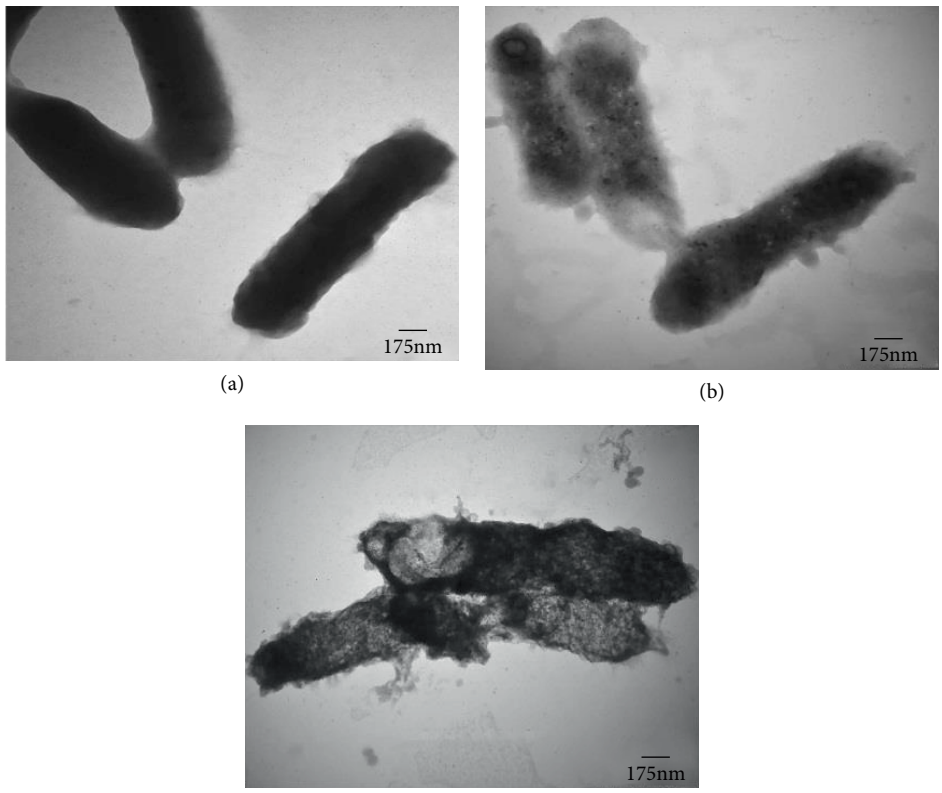

(a) (b) (c)

Figure 13: Effect on cellular morphology of PDR *E. coli* after treatment with CS-NPs coated TiO_2 NPs at various interval of time by TEM microscopy. (a) control, (b) 3 hrs of incubation, (c) 6 hrs of incubation.

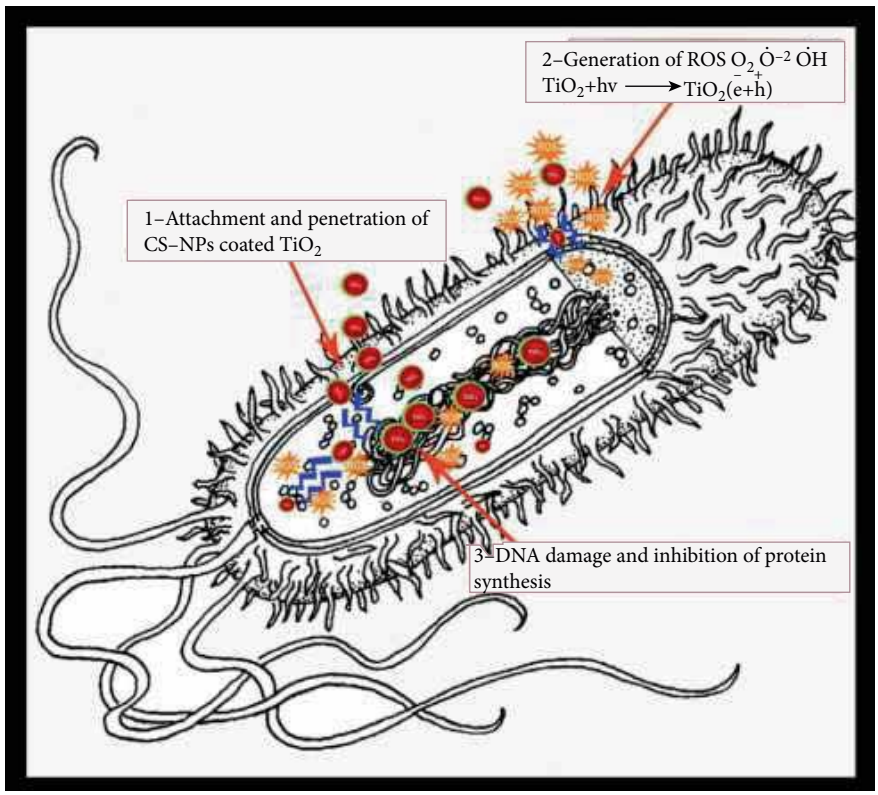

Figure 14: Proposed antibacterial mechanism of action of CS NPs coated TiO_2 NPs.

nanoparticles. The spherical shaped CS-NPsTiO_2 NPs was evident from SEM images. The corresponding formation mechanism of CS NPs coated TiO_2 NPs with chitosan was affirmed by various stretching and bending modes of the FTIR spectra. The band gap has been obtained in terms of F(R) values by the application of Kubelka-Munk function. The band gap has been workout from the Tauc plot, TiO_2NPs provides the band gap energy as 3.28 eV while CS-NPs coated TiO_2 NPs showing wider band gap 3.9 eV, making it more efficient antimicrobial agent. The elemental composition of CS-NPs coated TiO_2 NPs confirms the presence of major elements, carbon, oxygen and TiO_2 by EDX analysis. Present evaluation further confirmed coating of TiO_2 NPs with chitosan nanoparticles is found very effective as CS-NPs coated TiO_2 showed strong activity evident by increase in size of zone of inhibition. Synthesized CS-NPs coated TiO_2 was found bactericidal at MIC concentration of 0.78 μg/ml as lysed cells were observed by TEM these results closely linked with the antibacterial susceptibility tests and growth kinetic studies. The hemolytic and cytotoxicity studies of CS-NPs coated TiO_2 NPs showed its nontoxicity to the human cells. Hence stable, nontoxic and spherical shaped CS-NPs coated TiO_2 NPs were observed potential tool to kill an alarming pathogen i.e. PDR strain of *E. coli* in veterinary origin. CS-NPs coated TiO_2 NPs a competent option to customary, systemic antibiotic for controlling pathogens causing infection in the livestock animals.

Data Availability

The datasets generated during and/or analyzed during the current study are available from the corresponding author on reasonable request.

Conflicts of Interest

The authors declare that there is no conflicts of interest regarding the publication of this paper.

Acknowledgments

Authors would like to acknowledge the support provided by International Islamic University, Islamabad and NUST Research Directorate to conduct this research.

References

[1] M. Pol and P. L. Ruegg, "Treatment practices and quantification of antimicrobial drug usage in conventional and organic dairy farms in Wisconsin," *Journal of Dairy Science*, vol. 90, no. 1, pp. 249–261, 2007.

[2] J. A. Makovec and P. L. Ruegg, "Results of milk samples submitted for microbiological examination in Wisconsin from 1994 to 2001," *Journal of Dairy Science*, vol. 86, no. 11, pp. 3466–3472, 2003.

[3] F. Yang, L. H. Liu, X. P. Li et al., "Short communication: N-acetylcysteine-mediated modulation of antibiotic susceptibility of bovine mastitis pathogens," *Journal of Dairy Science*, vol. 99, no. 6, pp. 4300–4302, 2016.

[4] P. Desmarchelier and N. Fegan, *Pathogens in Milk Escherichia coli, Encyclopedia of Dairy Sciences*, Academic Press, London, UKpp. 60–66, 2nd edition, 2011.

[5] J. F. Acar and G. Moulin, "Integrating animal health surveillance and food safety: the issue of antimicrobial resistance," *Scientific and Technical Review OIE*, vol. 32, no. 2, pp. 383–392, 2013.

[6] M. Souli, I. Galani, and H. Giamarellou, "Emergence of extensively drug-resistant and pan drug-resistant gram-negative bacilli in Europe," *Eurosurveillance*, vol. 13, no. 47, p. 19045, 2008.

[7] H. M. M. Ibrahim, A. M. Ahmed, Y. Y. El-seedy, and S. A. El-Khodery, "Distribution of multidrug-resistant gram negative bacteria causing clinical mastitis in dairy cows," *Global Veterinaria*, vol. 15, pp. 268–277, 2015.

[8] A. Muñoz-Bonilla and M. Fernández-García, "Polymeric materials with antimicrobial activity," *Progress in Polymer Science*, vol. 37, no. 2, pp. 281–339, 2012.

[9] H. Palza, "Antimicrobial polymers with metal nanoparticles," *International Journal of Molecular Sciences*, vol. 16, no. 1, pp. 2099–2116, 2015.

[10] H. Wang, J. Qian, and F. Ding, "Emerging chitosan-based films for food packaging applications," *Journal of Agricultural and Food Chemistry*, vol. 66, no. 2, pp. 395–413, 2018.

[11] E. Tabesh, H. Salimijazi, M. Kharaziha, and M. Hejazi, "Antibacterial chitosan-copper nanocomposite coatings for biomedical applications," *Mater Materials Today: Proceedings*, vol. 5, no. 7, pp. 15806–15812, 2018.

[12] F. Wahid, J.-J. Yin, D.-D. Xue et al., "Synthesis and characterization of antibacterial carboxymethyl Chitosan/ZnO nanocomposite hydrogels," *International Journal of Biological Macromolecules*, vol. 88, pp. 273–279, 2016.

[13] A. Montaser, A. R Wassel, and O. N. Al-Shaye'a, "Synthesis, characterization and antimicrobial activity of schiff bases from chitosan and salicylaldehyde/TiO_2 nanocomposite membrane," *International Journal of Biological Macromolecules*, vol. 124, pp. 802–809, 2019.

[14] T. Matsunaga, R. Tomoda, T. Nakajima, and H. Wake, "Photoelectrochemical sterilization of microbial cells by semiconductor powders," *FEMS Microbiology Letters*, vol. 29, no. 1-2, pp. 211–214, 1985.

[15] J. Prakash, J. C. Pivin, and H. C. Swart, "Noble metal nanoparticles embedding into chitosan materials: from fundamentals to applications," *Advances in Colloid and Interface Science*, vol. 226, pp. 187–202, 2015.

[16] X. Zhang, G. Xiao, Y. Wang, Y. Zhao, H. Su, and T. Tan, "Preparation of chitosan-TiO_2 composite film with efficient antimicrobial activities under visible light for food packaging applications," *Carbohydrate Polymers*, vol. 169, pp. 101–107, 2017.

[17] M. Nasrollahzadeh, M. Atarod, B. Jaleh, and M. Gandomirouzbahani, "In situ green synthesis of Ag nanoparticles on graphene oxide/TiO_2 nanocomposite and their catalytic activity for the reduction of 4-nitrophenol, congo red and methylene blue," *Ceramics International*, vol. 42, no. 7, pp. 8587–8596, 2016.

[18] S. Subhapriya and P. Gomathipriya, "Green synthesis of titanium dioxide (TiO_2) nanoparticles by *Trigonellafoenum-graecum* extract and its antimicrobial properties," *Microbial Pathogenesis*, vol. 116, pp. 215–220, 2018.

[19] A. Rani, N. Zahirah, K. Husain, and E. Kumolosasi, "Moringa genus: a review of phytochemistry and pharmacology," *Frontiers in Pharmacology*, vol. 9, p. 108, 2018.

[20] R. S. Rossi, A. F. Amarante, L. B. Correia et al., "Diagnostic accuracy of Somatic cell, California Mastitis Test, and microbiological examination of composite milk to detect Streptococcus agalactiae intramammary infections," *Journal of Dairy Science*, vol. 101, no. 11, pp. 10220–10229, 2018.

[21] Eucast, "European committee on antimicrobial susceptibility testing. breakpoint tables for interpretation of MICs and zone diameters version 6.0," 2016.

[22] CLSI, "Performances Standards for Antimicrobial Susceptibility Testing; Twenty-Fourth Informational Supplement. M100–S26," Clinical Laboratory Standards Institute, Wayne, PA, USA, 2016.

[23] B. Jamil, R. Abbasi, S. Abbasi et al., "Encapsulation of cardamom essential oil in chitosan nano-composites: in-vitro efficacy on antibiotic-resistant bacterial pathogens and cytotoxicity studies," *Frontiers in Microbiology*, vol. 7, p. 1580, 2016.

[24] M. G. Guzmán, J. Dille, and S. Godet, "Synthesis of silver nanoparticles by chemical reduction method and their antibacterial activity," *International Journal of Chemical and BiomolecularEngineering*, vol. 2, no. 3, pp. 104–111, 2009.

[25] S. A. Holowachuk, M. F. Bal'a, and R. K. Buddington, "A kinetic microplate method for quantifying the antibacterial properties of biological fluids," *Journal of Microbiological Methods*, vol. 55, no. 2, pp. 441–446, 2003.

[26] M. Hartmann, M. Berditsch, J. Hawecker, M. F. Ardakani, D. Gerthsen, and A. S. Ulrich, "Damage of the bacterial cell envelope by antimicrobial peptides gramicidin S and PGLa as revealed by transmission and scanning electron microscopy," *Antimicrobial Agents and Chemotherapy*, vol. 54, no. 8, pp. 3132–3142, 2010.

[27] A. R. Lupu and T. Popescu, "The noncellular reduction of MTT tetrazolium salt by TiO_2 nanoparticles and its implications for cytotoxicity assays," *Toxicology in Vitro*, vol. 27, no. 5, pp. 1445–1450, 2013.

[28] J. Choi, V. Reipa, V. M. Hitchins, P. L. Goering, and R. A. Malinauskas, "Physicochemical characterization and in vitro hemolysis evaluation of silver nanoparticles," *Toxicological Sciences*, vol. 123, no. 1, pp. 133–143, 2011.

[29] B. X. Lei, Q. P. Luo, X. Y. Yu, W. Q. Wu, C. Y. Su, and D. B. Kuang, "Hierarchical TiO_2 flowers built from TiO_2 nanotubes for efficient Pt-free based flexible dye-sensitized solar cells," *Physical Chemistry Chemical Physics*, vol. 14, no. 38, pp. 13175–13179, 2012.

[30] E. S. Tang, K. M. Huang, and L. Y. Lim, "Ultrasonication of chitosan and chitosan nanoparticles," *International Journal of Pharmaceutics*, vol. 265, no. 1-2, pp. 103–114, 2003.

[31] R. Saravanan, J. Aviles, F. Gracia, E. Mosquera, and V. K. Gupta, "Crystallinity and lowering band gap induced visible light photocatalytic activity of TiO_2/CS (chitosan) nanocomposites," *International Journal of Biological Macromolecules*, vol. 109, pp. 1239–1245, 2018.

[32] G. Alagumuthu and T. Anantha Kumar, "Synthesis and characterization of Chitosan/TiO_2 nanocomposites using liquid phase deposition technique," *International Journal of Nanoscience and Nanotechnology*, vol. 4, pp. 105–111, 2013.

[33] B. Lin, Y. Du, X. Liang, X. Wang, X. Wang, and J. Yang, "Effect of chitosan coating on respiratory behavior and quality of stored litchi under ambient temperature," *Journal of Food Engineering*, vol. 102, no. 1, pp. 94–99, 2011.

[34] B. F. Lin, W. Wang, Y. M. Li, X. Q. Liang, and Y. M. Du, "Conversion of chitosan to facilitate preparation of chitosan carboxylic salt with moisture absorption-retention abilities In Advanced Materials Research," *Trans Tech Publications*, vol. 396, pp. 2193–2197, 2012.

[35] B. Lin, Y. Luo, Z. Teng, B. Zhang, B. Zhou, and Q. Wang, "Development of silver/titanium dioxide/chitosan adipate nanocomposite as an antibacterial coating for fruit storage," *LWT — Food Science and Technology*, vol. 63, no. 2, pp. 1206–1213, 2015.

[36] B. Shams, N. G. Ebrahimi, and F. Khodaiyan, "Development of antibacterial nanocomposite: whey protein-gelatin-nanoclay films with orange peel extract and tripolyphosphate as potential food packaging," *Advances in Polymer Technology*, vol. 2019, pp. 1–9, 2019.

[37] L. K. Adams, D. Y. Lyon, and P. J. Alvarez, "Comparative eco-toxicity of nanoscale TiO_2, SiO_2, and ZnO water suspensions," *Water Research*, vol. 40, pp. 3527–3532, 2006.

[38] T. Z. Tong, C. T. Binh, J. J. Kelly, J. F. Gaillard, and K. A. Gray, "Cytotoxicity of commercial nano-TiO_2 to *Escherichia coli* assessed by high-throughput screening: effects of environmental factors," *Water Research*, vol. 47, no. 7, pp. 2352–2362, 2013.

[39] B. Sha, W. Gao, S. Wang, F. Xu, and T. Lu, "Cytotoxicity of titanium dioxide nanoparticles differs in four liver cells from human and rat," *Composites Part B: Engineering*, vol. 42, no. 8, pp. 2136–2144, 2011.

[40] T. M. Crizel, A. O. Rios, V. D. Alves, N. Bandarra, M. Moldão-Martins, and S. H. Flôres, "Active food packaging prepared with chitosan and olive pomace," *Food Hydrocolloids*, vol. 74, pp. 139–150, 2018.

[41] C. Vilela, R. J. B. Pinto, J. Coelho et al., "Bioactive chitosan/ellagic acid films with UV-light protection for active food packaging," *Food Hydrocolloids*, vol. 73, pp. 120–128, 2017.

[42] H. A. Foster, I. B. Ditta, and S. A. Varghese, "Photocatalytic disinfection using titanium dioxide: spectrum and mechanism of antimicrobial activity," *Applied Microbiology and Biotechnology*, vol. 90, no. 6, pp. 1847–1868, 2011.

[43] L. Wang, C. Hu, and L. Shao, "The antimicrobial activity of nanoparticles: present situation and prospects for the future," *International Journal of Nanomedicine*, vol. 12, pp. 1227–1249, 2017.

[44] Z. Zhu, H. Cai, and D. W. Sun, "Titanium dioxide (TiO_2) photocatalysis technology for nonthermal inactivation of microorganisms in foods," *Trends in Food Science & Technology*, vol. 75, pp. 23–35, 2018.

[45] H. Nikaido, "Outer membrane, Gram-negative bacteria," in *Encyclopedia of Microbiology*, M. Schaechter, Ed., pp. 439–452, Academic Press, San Diego, CA, USA, 3rd edition, 2009.